International Journal of ChemTech Research
CODEN(USA): IJCRGG ISSN : 0974-4290
Vol.5, No.3, pp 1152-1161, April-June 2013

IPACT-2013[14th – 15th March 2013]
National Conference on Industrial Pollution And Control Technology-2013

Electrocatalyzed Oxidation of Methanol on Carbon Supported Platinum Electrode in Membraneless Sodium Percarbonate Fuel Cells (MLSPCFC)

A. Arun[1]*, M. Gowdhamamoorthi[2], S. Kiruthika[3] and B. Muthukumaran[4*]

[1, 2, 4] **Department of Chemistry, Presidency College, Chennai – 600 005, India,**

[3] **Department of Chemical Engineering, SRM University, Chennai – 603 203, India.**

Corres.author: arunmscphd@gmail.com
Tel.: +91-44-28544894; Fax: +91-44-28510732.

Abstract: This paper presents the development of a novel liquid-based microscale fuel cell using sodium percarbonate in alkaline medium that utilizes the occurrence of laminar flows in an E-shaped microchannel to keep the separation of fuel and oxidant streams without turbulent mixing. The liquid fuel and oxidant streams enter the system at different inlets, and then merge and flow in parallel to one another through the channel between two electrodes without the need of a membrane to separate both streams. Thus developed fuel cell is based on a membraneless structure. In this membraneless fuel cell, methanol and sodium percarbonate were used as a fuel at anode and an oxidant at cathode respectively. Operating a fuel cell under alkaline conditions has positive effects on the reaction kinetics, both at the anode and cathode, while the cell performance 'mixed-media' conditions offers an opportunity to increase the maximum achievable open cell potential (OCP). With a fuel mixture flow rate of 100 µl min^{-1}, a maximum output power density of 26.76 mW cm^{-2} was achieved. The developed fuel cell features has no proton exchange membrane and simple planar structure, which enables high design flexibility and easy integration of the portable power applications.
Keywords: Membraneless. Microfluidic. Sodium percarbonate fuel cell (MLSPCFC). Fuel cell in alkaline medium. Portable power applications.

Introduction

A membraneless fuel cell based on microfluidic device has received much attention due to its wide applications in portable power sources such as cellphones, laptop computers, and many specialized devices such as remote sensors, diagnostic tests, and global positioning systems and microelectromechanical systems (MEMS)[1-3]. A membraneless fuel cell is defined as a fuel cell with liquid delivery and removal, reaction sites and electrode structures all within bounds to a microfluidic channel. The concept of a membraneless fuel cell was first manifested by Ferrigno et al.[4] with a vanadium redox fuel cell. This type of fuel cell can operates without a

physical barrier, such as a membrane, to separate the anode and cathode, and can use both metallic and biological catalysts[5]. And Chen et al[6]. performed an analytic study of the planar channel design and found that the device behavior and performance were comparable to the Y-channel designs. They concluded that a better method for improving laminar flow based fuel cell performance is needed than more increasing the electrode surface area. The fuel cell consisting of the membrane electrode assembly (MEA) comprises the electrodes and membrane, and accounts for around 50% of the total cost[7]. Furthermore the overall structure of a microscale fuel cell becomes more complicated when there is a membrane for the segregation of fuel and oxidant[8]. During the past years, portable versions of fuel cells have emerged. The most promising miniature fuel cell is membraneless methanol fuel cell (MLMFC), which is convenient and has a reasonable electrochemical performance and does not require MEAs. In recent years Choban et al[9] studied the effect of operating laminar flow based fuel cells in all acidic, all alkaline, and acidic/alkaline medium and concluded that a fuel cell in alkaline medium can give 40% efficiency than in acidic medium. Since certain hydrocarbons such as methanol and formic acid can easily be stored in liquid form under ambient conditions are known to give safer high energy densities. And also methanol is a cheap and can easily be obtained from fossil fuels, such as natural gas or coal, as well as from existence sources through fermentation of agricultural products and from biomasses. Many works are under progress on the development of microfluidic direct methanol fuel cells[10-13]. In this work also we use methanol as our fuel. Since energy is stored as a reservoir of fuel rather than as an integral part of the power source, and due to continuous operation capability by refueling[14], fuel cells have numerous advantages over batteries. In previous years, direct liquid fuel cells or hydrogen fuel cells operating in acidic media have been extensively studied, but those operating in alkaline media have received much less attention although both fuel oxidation at the anode[15] especially CO oxidation[16] and the oxygen reduction reaction at the cathode[17,18] studies indicates that the reaction kinetics are more easily achieved in alkaline medium; And also the fuel cell in alkaline medium has one more advantage that any carbonates formed when operating in alkaline media are immediately removed by the flowing electrolyte[19]. Therefore in our study we use methanol as a fuel in alkaline medium to improve the performance of membraneless fuel cells as well.

Results and Discussion

In a liquid system, the cell performance will be pretended, if the continuous flow of liquid were to diffuse all the way from the liquid-liquid interface to the opposing electrode. This is known as fuel crossover that creates mixed potentials, which leads to decrease in cell efficiency[20]. But in membraneless fuel cell system, all liquid design eliminates issues related to fuel crossover, anode dry-out, and cathode outpouring[21,22]. In addition, lack of a membrane also allows for operation of laminar flow based fuel cells in alkaline medium. At cathode for constant conditions, the increase in fuel concentration to the anode has shown a limited effect on cell performance[23,24]. However, in this work, we selected methanol a higher energy density over formic acid as a fuel, which is a very important factor in portable applications[25]. Fig.1 shows the Cell potential (V) Vs Current density (mA/cm^2) and current density (mA/cm^2) Vs power density (mW/cm^2) curves for different methanol concentrations between 1 and 5 M respectively.

Fig 1: **1.a**

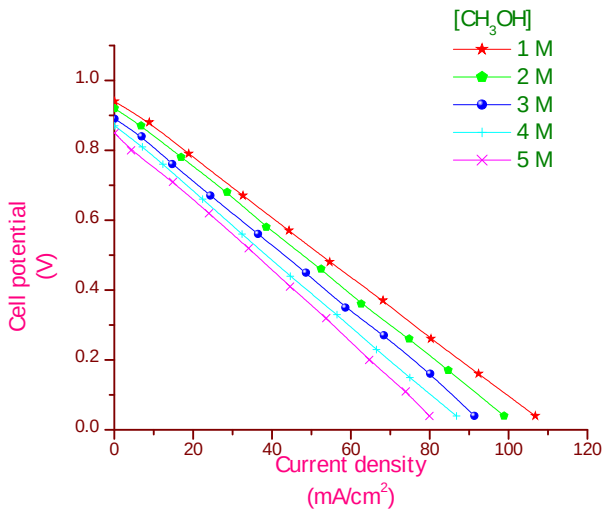

1.b

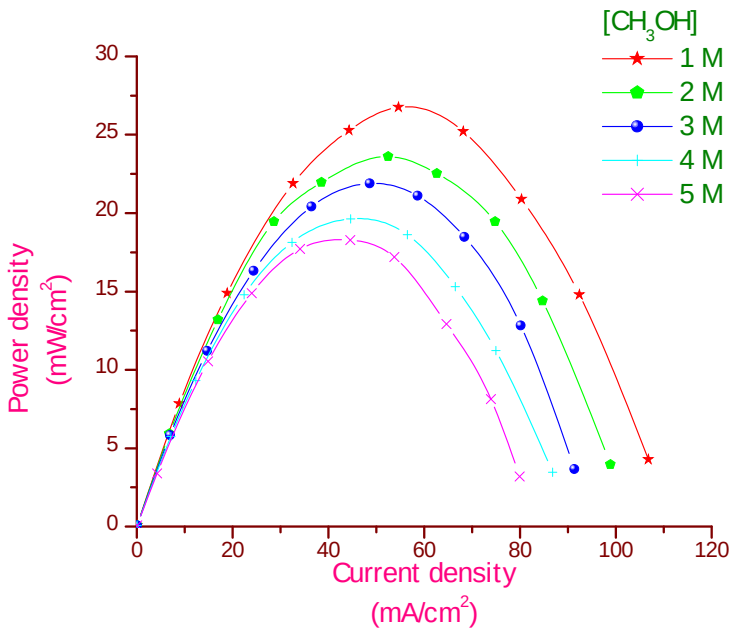

Fig.1 Variations of cell performance with five assigned concentrations of Methanol [CH_3OH] *(a)* the polarisation curves; *(b)* the corresponding power density curves

The experimental results show that the fuel cell performance increases initially and decreases as the methanol concentration increases. This decreasing trend in cell performance at higher methanol concentrations can be explained in four capable reasons: a) creation of mixed potential at the cathode due to fuel crossover; b) kinetic decrease in anode; c) transport resistance increase at the anode; d) Ohmic resistance increase. As mentioned above, fuel crossover will not be present in any membraneless fuel cell; therefore higher methanol concentration is not the cause for decrease of performance in fuel cell. The kinetic decrease in anode also cannot be the reason because the electro-oxidation of methanol on Pt has a positive reaction order between 0.5 and 1 M. Thus, the activity at the anode increases initially as the concentration of fuel increases. Therefore, the anode is not limited by kinetic performance with higher methanol concentrations. An increase in Ohmic resistance can happen when mass transport resistance create a higher driving force for the methanol to diffuse across the depletion boundary layer to the electrode. Therefore, the protons cannot be transported efficiently and this leads to a poor cell performance, is the only explanation for having decreased cell performance with the higher methanol concentrations. For instance, at 0.5 M methanol solution, the mobility of proton is about 3.6×10^{-3} ($cm^2/(s.V)$) and at 4 M methanol solution, the mobility of proton decreases to about 2.7×10^{-3} ($cm^2/(s.V)$)[26]. The typical open circuit potentials (OCPs) reported for miniaturized direct methanol fuel cells (e.g., DMFCs) range from 0.5 to 0.8 V[27]. While the OCPs obtained in this work is significantly higher 0.94 V for 1 M methanol in an alkaline medium.

The membraneless fuel cell design also offers the following advantages: a) water management issues can be avoided by the continuous flow of aqueous electrolyte b) without any change to the cell other than the pH of the streams each membraneless fuel cell can be operated either in alkaline or in acidic medium[28]. In alkaline medium, the methanol oxidation starts at a much lower potential than in acidic medium. Moreover, the current densities due to methanol oxidation in alkaline medium are higher than in acidic medium. This observation of superior methanol oxidation in alkaline medium is in contract with electrochemical studies by Tripkovic et al[29,30]. In this work we use 1 M potassium hydroxide (KOH) solution as an alkaline medium at cathode. Finally, the high open circuit potential of the membraneless fuel cell in alkaline medium eliminates the need for the development of an appropriate polymer electrolyte membrane that allows hydroxyl ions to diffuse across.

Since Sodium percarbonate (SPC) is a convenient source of hydrogen peroxide[31,32]. We introduce sodium percarbonate, ($2Na_2CO_3 \cdot 3H_2O_2$) as an oxidant in this work.

$$2Na_2CO_3.3H_2O_2 \rightarrow 2Na_2CO_3 + 3H_2O_2 \quad (1)$$

In an alkaline medium, the electron-losing reaction of H_2O_2 proceeds in two steps, the first being

$$H_2O_2\,(aq) + OH^-\,(aq) \rightarrow HO_2^-\,(aq) + H_2O \quad (2)$$

which is the acid-base reaction between the weak acid, H_2O_2, and the alkaline electrolyte. The second is

$$HO_2^-\,(aq) + OH^-\,(aq) \rightarrow O_2 + H_2O + 2e^- \quad (3)$$

When the concentration of oxidant is increased, the cell potential also increases gradually and reaches the maximum of 0.94 V at about 0.1 M Sodium percarbonate as shown in Fig.2.

2.a

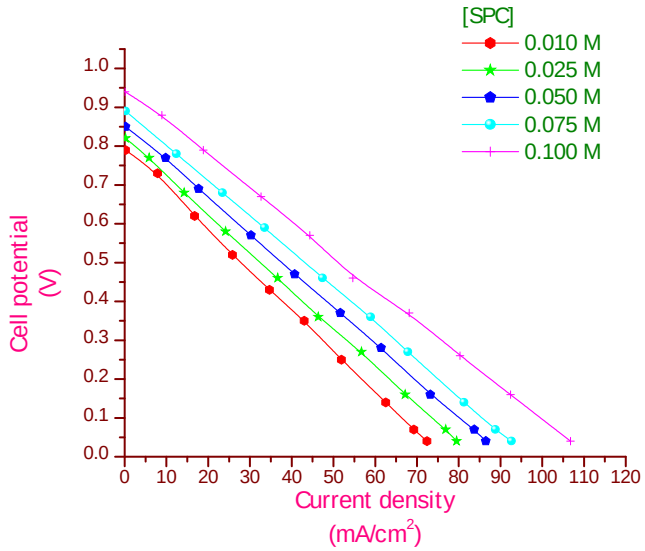

2.b

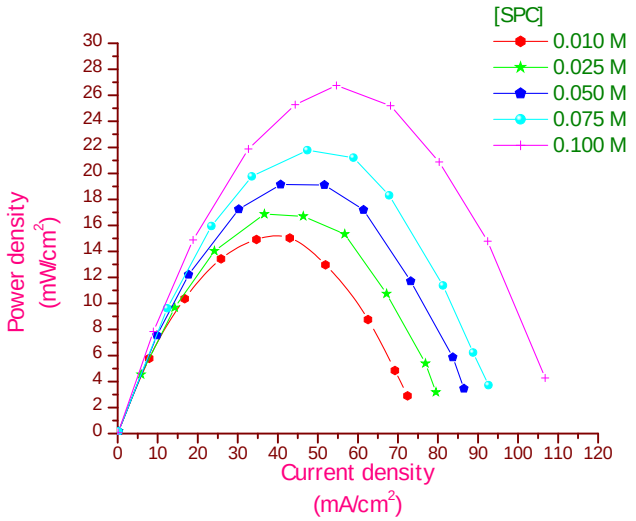

Fig.2 : Variations of cell performance with five assigned concentrations of Sodium percarbonate [SPC] (a) the polarisation curves; *(b)* the corresponding power density curves

The study of reactant composition

To determine the resource composition of a fuel mixture the effect of reactant concentration on the fuel cell output was studied experimentally. More number of combinations of reactant concentration were applied: five fuel concentrations were applied as 1, 2, 3, 4 and 5 M; five oxidant concentrations were applied as 0.010, 0.025, 0.050, 0.075 and 0.1 M and six electrolyte concentrations were applied as 0.10, 0.25, 0.50, 0.75, 1, and 2 M. All possible combinations were applied except 0 M oxidant and 0 M electrolyte because the fuel cell output could not be stable without such reactants.

The current-voltage (I-V) measurement was carried out with different external loads to determine the resource composition of a fuel mixture. 20 mm distance was maintained between the anode and cathode. The obtained maximum power densities with respect to the applied combinations of reactant concentration are presented in Fig. 3.

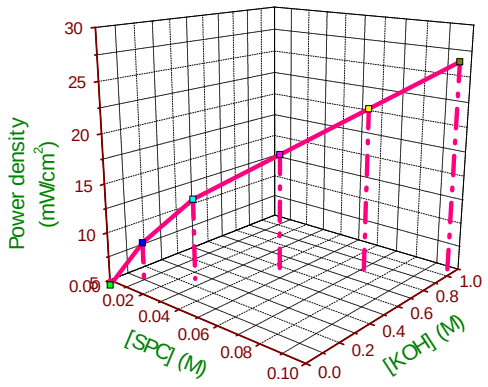

Fig. 3 Effect of various combinations of reactant concentrations on the maximum output power density.

If the concentration of electrolyte is increased, the maximum power density also increases. Thus the highest output power density (26.76 mW cm^{-2}) and highest output current density (106.78 mA cm^{-2}) was achieved with the fuel mixture of 1 M methanol, 0.1 M sodium percarbonate and 1 M hydroxyl ions. However, this dependence became weak for fuel concentrations larger than 1 M. By considering the magnitude and stability of the fuel cell output, the resource composition of a fuel mixture was determined to be 1 M methanol, 0.1 M sodium percarbonate and 1 M hydroxyl ions.

The distance effect on the fuel cell output

Based on the resource fuel mixture, in order to find the potential benefit from a reduced diffusion length of reacting species moving between the anode and cathode the macroscale fuel cell test was conducted for different distances between 1 to 100 mm. The cell potential and current were measured with various load resistances for different distances between the anode and cathode. When the distance between the anode and cathode decreased, the maximum power density increased as shown in Fig. 4.

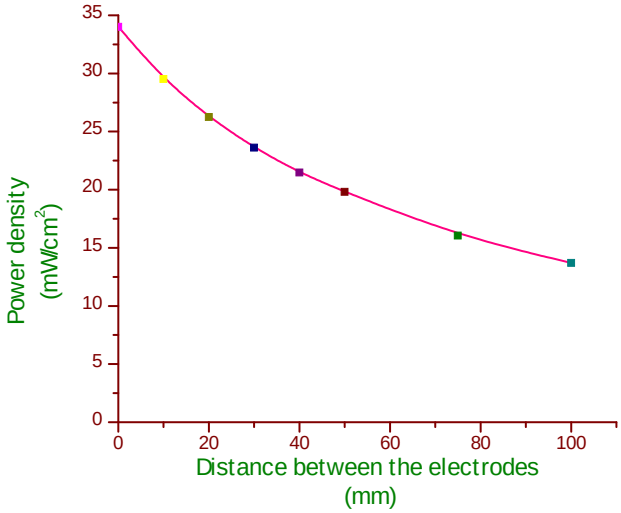

Fig. 4 Effect of distance between anode and cathode on the fuel cell output power density.

Considering the role of a charge carrier, a shorter diffusion length is believed to give a faster electrochemical reaction because the diffusion time of reacting species would be shorter. Therefore, more reactions can take place at a given time, which increases the total number of charges involving the electrochemical reactions at the anode and cathode. This finding provides a good evidence of the presence of a charge carrier moving between the anode and cathode in the fuel mixture to complete redox reactions of the fuel cell[33].

Microscale fuel cells

Depending on the distance effect demonstrated at the macroscale level, a microscale fuel cell was developed in order to further extend the distance effect to a microscale level that enables microscale diffusion lengths of reacting species. Four different designs of the microscale fuel cell were prepared to examine the distance effect between the anode and cathode on the fuel cell output. In addition, the microfluidic behavior of the microscale fuel cell was characterized under different fuel mixture flow rates.

Design considerations

The developed microscale fuel cell is based on a planar and membraneless structure. Thus, electrodes can be arranged on the same plane without a proton exchange membrane, so that the fuel cell dimensions can be flexibly adjusted to meet specific design needs. For a planar arrangement, microelectrodes were employed as anode and cathode and the spacing between anode and cathode was determined by photolithography. Four different distances between anode and cathode, 10, 20, 50, and 100 mm, were prepared and tested for comparison. In each design, the anode and cathode area was unchanged to 0.026 cm^2.

Construction of the fuel cell

In this study, we used a novel fuel cell consisting of a E-shaped laminar flow channel with electrodes on the inner sidewalls of the main channel was typically constructed by using standard diplomatic occasions. In our microfluidic fuel cell construction, catalyst-coated graphite plates of 1mm *(*Graphite India., poco grade EDM-3, 0.0001 in. particle size*)* are employed to act as electrodes, current collectors, and channel structures as reported. Since, the reduced diffusion interface inherent in the side-by-side design reduces the amount of reactant wasted to the mixing region, these graphite plates are placed side by side with a specific spacing to form the length of the channel where the fuel and oxidant streams flow next to each other.

The inlets to this channel are milled out of the graphite plates with a drill bit at desired dimensions, typically 0.250 mm. Before assembling the fuel cell, platinum black catalyst is applied on both the inner sidewalls of the graphite plates by electrodeposition method[34]. Subsequent electrodeposition of catalyst to the cathode and anode, the E-shaped microfluidic channel structure is molded with PDMS poly *(*dimethylsiloxane*)*, typically 1–

10 mm in thickness and finally sealed with a solid substrate such as 2 mm-thick pieces of PMMA Poly *(*methylmethacrylate*)* to provide rigidity and supportive strength to the layered system Fig.5.

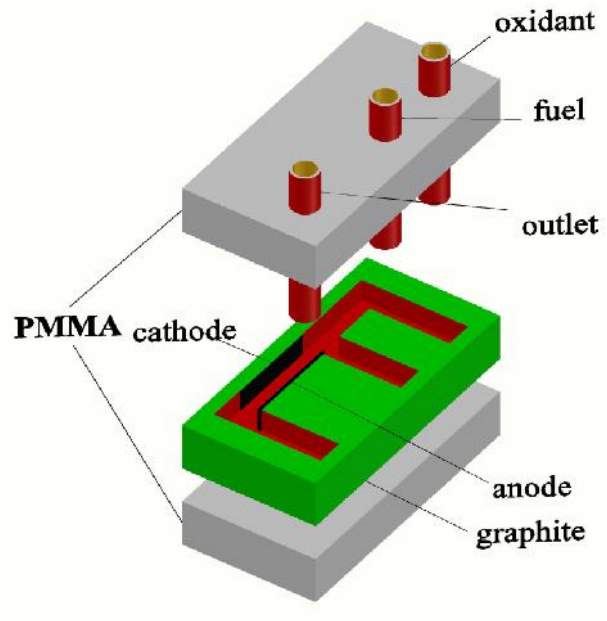

Fig.5 Schematic of the E-shaped membraneless laminar flow-based fuel cell with graphite plates molded with PDMS poly *(*dimethylsiloxane*)* and sealed with PMMA poly *(*methylmethacrylate*).*

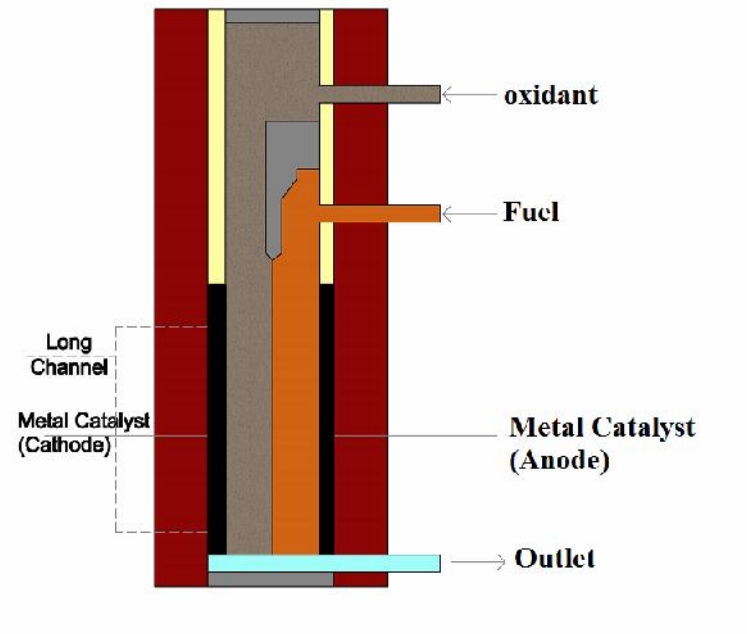

Fig.6 The side view of the E - type planar membraneless microfuel cell.

Silicon tubing *(*Instech Solomon *PE* = 205, I.D. 1.0 mm*)* is placed to guide the fuel and oxidant into the E-shaped channel systems at the top and to guide the waste stream out at the bottom of the channel. The tubing is inserted into holes that are punched exactly at the three ends of the E-shaped channel design and glued into place.

The fluid flow is regulated using a syringe pump with typical flow rates of ~100 μL min^{-1} per stream. Consequently, the microfluidic cell keeps these fluids stable without a separation membrane. A membrane, as used in MEAs, brings about a resistance to the transport of ions through the electrolytes. Furthermore, MEAs are expensive components at present. Therefore, the cell structure without the membrane has two merits, decrease of electrical resistivity in the cell and inexpensive material cost, apart from the problems associated with PEM-type fuel cells like fuel crossover [35], membrane degradation, a long startup time, ohmic losses, size, fabrication and water management limited durability of catalysts[36].

All experiments were conducted using methanol, CH_3OH in deionized water as a fuel and sodium percarbonate, ($2Na_2CO_3 \cdot 3H_2O_2$) *(*Riedel*)* in deionized water as the oxidant and potassium hydroxide, (KOH) *(*Merck AR Grade*)* in deionized water as an electrolyte. The experiments were conducted at room temperature with electrodeposited platinum black on both the electrodes. For fuel cell characterization the current and potential were measured at different loads using a variable resistor.

The effect of fuel mixture flow rate

Since maximum power density is also dependent on the transport time of reacting species it can be controlled by its flow rates. In this experiment, flow rates of 1, 10, 25, 50, 75, 100, 125, 150, 175 and 200 µl min^{-1} were tested. The cell potential and current were measured with different external loads as a function of the flow velocity of fuel mixture. Using the flow rate applied and the cross-sectional area of the channel a flow velocity can be calculated. Previous works have shown that the increased flow rate improves performance by increasing the reactant flux and by decreasing the concentration boundary layer thickness providing better reactant supply to the electrodes.

In this work, the maximum power density is obtained at about 100 µl min^{-1} after that the maximum power density decreases with increase in flow rate as shown in Fig. 7.

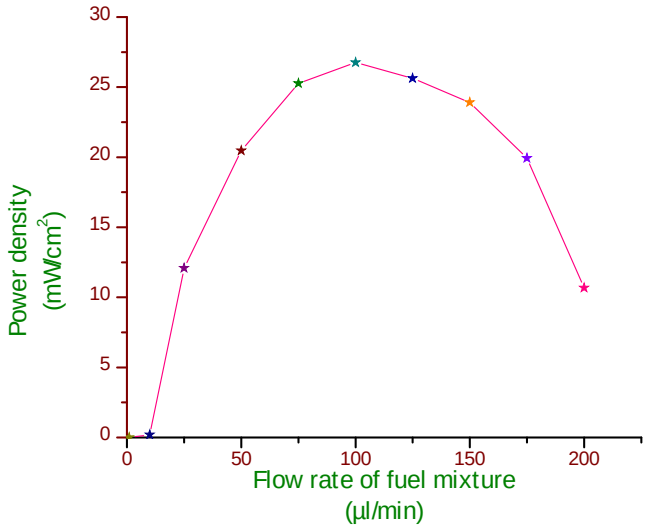

Fig. 7 Effect of flow rate of fuel mixture on the fuel cell output power density.

It is believed that more electrochemical reactions would take place at a given time and a greater output current could develop in the end.

Conclusions

The methanol and sodium percarbonate fuel cell was successfully developed and demonstrated in alkaline solution. Based on a membraneless structure in this fuel cell, a shorter distance between anode and cathode was shown to generate a maximum current density of about 106.78 mA/cm^2 and a maximum power density of about 26.76 mW/cm^2 with a fuel mixture flow rate of 100 µl min^{-1} was extracted. The maximum power density were obtained at a shorter distance between anode and cathode is due to a faster transport time of reacting species,

which results in more electrochemical reactions at a given time. The microscale fuel cell developed in this work has advantages over previously reported microscale direct methanol fuel cells by a simple planar structure, yielding a maximum output power density. Due to the simple structure of the developed fuel cells, the anode and cathode can be arranged on the same plane without a proton exchange membrane, which enables that the fuel cell dimensions can be flexible adjusted to meet specific design needs for the applications of microfluidic systems and portable power sources.

References

1. E. R. Choban, L. J. Markoski, A. Wieckowski, P. J. A. Kenis, J. Power Sources 128 (2004) 54-60.
2. J. L. Cohen, D. A. Westly, A. Pechenik, H. D. Abruna, J. Power Sources 139 (2005) 96-105.
3. A. Bazylak, D. Sinton, N. Djilali, J. Power Sources 143 (2005) 57-66.
4. R. Ferrigno, A. D. Stroock, T. D. Clark, M. Mayer and G. M. Whitesides, *J. Am. Chem. Soc.*, 124 (2002) 12930–12931.
5. E. Kjeang, Ned Djilali, D. Sinton, J. Power Sources 186 (2009) 353-369.
6. F. Chen, M. H. Chang and M. K. Lin, *Electrochim. Acta*, 52 (2007) 2506-2514.
7. H. Tsuchiya, O. Kobayashi, International Journal of Hydrogen Energy 29 (2004) 985-990.
8. J. -W. Choi, W. Sung, Technical Digest of the 13th International Conference on Solid-State Sensors, Actuators, and Microsystems, (2005) pp. 1852-1855.
9. E. R. Choban, J. S. Spendelow, L. Gancs, A. Wieckowski, and P. J. A. Kenis, *Electrochim. Acta, 50* (2005) 5390-5398.
10. G. Q. Lu, C. Y. Wang, T. J. Yen, X. Zhang, *Electrochim. Acta*, 49 (2004) 821.
11. S. Kelley, G. Deluga, W. H. Smyrl, *Electrochem. Solid-State Lett.* 3 (2000) 407.
12. T. Yen, N. Fang, X. Zhanga, G. Q. Lu, C. Y. Wang, Appl. Phys. Lett. 83 (2003) 4056.
13. S. Motokawa, M. Mohamedi, T. Momma, S. Shoji, T. Osaka, Electrochem. Commum. 6 (2004) 562.
14. R. F. Services, Science 296 (2002) 1222-1224.
15. A. V. Tripkovic, K. D. Popovic, B. N. Grgur, B. Blizanac, P. N. Ross, and N. M. Markovic, *Electrochim. Acta*, 47 (2002) 3707.
16. J. S. Spendlow, G. Q. Lu, P. J. A. Kenis and A. Wieckowski, *J. Electroanal Chem*, 568 (2004) 215.
17. A. J. Appleby, Energy, 11 (1986) 13.
18. K. F. Blurton and E. McMullin, Energy Convers, 9 (1969) 141.
19. R. S. Jayashree, D. Egas, J. S. Spendelow, D. Natarajan, L. J. Markoski, and P. J. A. Kenis, *Electrochem. Solid-State Lett*, 9 (5) (2006) A 252-A256.
20. J. D. Morse, *Int. J. Energy Res*, 31 (2007) 576-602.
21. E. R. Choban, P. Waszczuk, L. J. Markoski, A. Wieckowski, P. J. A. Kenis, Proceedings of the First International Conference on Fuel Cell Science Engineering and Technology, Rochester, NY, April (2003) 21-23.
22. E. R. Choban, L. J. Markoski, J. Stoltzfus, J. S. Moore, P. J. A. Kenis, Proceedings of the 40th Power Sources Conference, Cherry Hill, NJ, June (2002) 10-13.
23. B. Steele, A. Heinzel, Nature 414 (2001) 345.
24. J. Yeom, J. S. Ranga, G. Z. Mozsgai, A. Asthana, E. R. Choban, M. Mitchell, P. J. A. Kenis, M. A. Shannon, Hilton Head 2004, A solid state sensor, actuator and Microsystems workshop, Hilton Head Island, SC, June (2004) 6-10.
25. I. B. Sprague, P. Dutta, and S. Ha, J. Power and Energy, 223 Part A (2009) 799-808.
26. J. Bockris, and A. K. N. Reddy, Modern electrochemistry: an introduction to an interdisciplinary area, Plenum Press, NY, (1970) pp. 470-474.
27. T. Shimizu, T. Momma, M. Mohamedi, T. Osaka, And S. Sarangapani, J. Power Sources, 137 (2004) 277.
28. J. L. Cohen, D. J. Volpe, D. A. Westly, A. Pechenik, and H. D. Abruna, Langmuir, 21 (2005) 3544.
29. A. V. Tripkovic, S. Strbac, and K. D. Popovic, *Electrochem. Commun*. 5 (2003) 484.
30. A. V. Tripkovic, K. D. Popovic, J. D. Lovic, V. M. Jovanovic, and A. Kowal, *J. Electroanal Chem*, 572 (2004) 119.
31. F. A. Cotton, G. Wilkinson, "Advanced inorganic chemistry", *Wiley Interscience, New York,(* 1988) 812.
32. C. Karunakaran, R. Kamalam, "Structure-reactivity correlation of anilines in acetic acid", *J. Org. Chem.*, vol.67 (Feb 2002) pp.1118-24.

33. W. Sung, J.-W. Choi, J. Power Sources, 172 (2007) 198-208.
34. M. P. Maher, J. Pine, J. Wright, Y. Tai, J Neurosci Methods, 87 (1999) 45.
35. L. Carrette, K. A. Friedrich, U. Stimming, Chem Phys Chem, 1 (2000) 162.
36. M. Eikerling, A. A. Kornyshev, A. M. Kuznetsov, J. Ulstrup, S. Walbran, J Phys Chem B 105 (2001) 3646.

*****